frontiers in Physics

REVIEW
published: 30 September 2021
doi: 10.3389/fphy.2021.633848

Actuators for MRE: New Perspectives With Flexible Electroactive Materials

Jean-Lynce Gnanago[1], *Jean-Fabien Capsal*[2], *Tony Gerges*[1], *Philippe Lombard*[1], *Vincent Semet*[1], *Pierre-Jean Cottinet*[2], *Michel Cabrera*[1] *and Simon Auguste Lambert*[1]*

[1]*Université de Lyon, INSA Lyon, Université Claude Bernard Lyon 1, Ecole Centrale de Lyon, CNRS, Ampère UMR5005, Villeurbanne, France,* [2]*EA682 Laboratoire de Génie Electrique et Ferroélectricité, Institut National des Sciences Appliqué, Villeurbanne, France*

Since 1995, Magnetic Resonance Elastography (MRE) has been constantly developed as a non-invasive diagnostic tool for quantitative mapping of mechanical properties of biological tissues. Indeed, mechanical properties of tissues vary over five orders of magnitude (the shear stiffness is ranging from 10^2 Pa for fat to 10^7 Pa for bones). Additionally, these properties depend on the physiological state which explains the granted benefit of MRE for staging liver fibrosis and its potential in numerous medical and biological domains. In comparison to the other modalities used to perform such measurement, Magnetic Resonance (MR) techniques offer the advantages of acquiring 3D high spatial resolution images at high penetration depth. However, performing MRE tissue characterization requires low frequency shear waves propagating in the tissue. Inducing them is the role of a mechanical actuator specifically designed to operate under Magnetic Resonance Imaging (MRI) specific restrictions in terms of electromagnetic compatibility. Facing these restrictions, many different solutions have been proposed while keeping a common structure: a vibration generator, a coupling device transmitting the vibration and a piston responsible for the mechanical coupling of the actuator with the tissue. The following review details the MRI constraints and how they are shaping the existing actuators. An emphasis is put on piezoelectric solutions as they solve the main issues encountered with other actuator technologies. Finally, flexible electroactive materials are reviewed as they could open great perspectives to build new type of mechanical actuators with better adaptability, greater ease-of-use and more compactness of dedicated actuators for MRE of small soft samples and superficial organs such as skin, muscles or breast.

Keywords: magnetic resonance imaging, actuators, electroactive materials, magnetic resonance elastography, piezoelectricity

OPEN ACCESS

Edited by:
Jean-Luc Gennisson, Laboratoire d'imagerie biomédicale Multimodale Paris-Saclay (BioMaps), France

Reviewed by:
Ingolf Sack, Charité—Universitätsmedizin Berlin, Germany
Najat Salameh, University of Basel, Switzerland

***Correspondence:**
Simon Auguste Lambert
simon.lambert@univ-lyon1.fr

Specialty section:
This article was submitted to Medical Physics and Imaging, a section of the journal Frontiers in Physics

Received: *26 November 2020*
Accepted: *20 September 2021*
Published: *30 September 2021*

Citation:
Gnanago J-L, Capsal J-F, Gerges T, Lombard P, Semet V, Cottinet P-J, Cabrera M and Lambert SA (2021) Actuators for MRE: New Perspectives With Flexible Electroactive Materials. Front. Phys. 9:633848. doi: 10.3389/fphy.2021.633848

INTRODUCTION

For a long time, physicians have been using palpation to detect diseases revealed by qualitative changes of tissue stiffness. In parallel, the development of quantitative methods to assess mechanical properties of living tissues at different spatial scales and their link with physiopathological states of tissues have been constantly investigated [1–3]. Indeed, mechanical properties of tissues vary over five orders of magnitude (the shear stiffness is ranging from 10^2 Pa for fat to 10^7 Pa for bones). Additionally, these properties depend on the physiological state which explains the granted benefit of Magnetic Resonance Elastography (MRE) for staging liver fibrosis and its potential in numerous medical and biological domains [4]. For instance it has been shown that extracellular matrix, i. e the

biochemical and mechanical micro-environment of tumors, is a key determinant in the metastatic process [5].

In the last decades, different imaging modalities such as ultrasound [6], magnetic resonance imaging (MRI) [1], or even optical coherence tomography [7] have been adapted to quantitatively map the mechanical properties of tissues. Today, one dimensional (1D) ultrasound elastography is used in clinical routine to non-invasively diagnose and classify patients with liver fibrosis [8]. Two-dimensional (2D) shear wave ultrasound imaging has demonstrated various benefits to diagnose for instance chronic liver diseases [9], or breast tumors [6]. Finally MRE has the potential of characterizing *in vivo* the mechanical properties of various tissues in 3D and has been approved by the Food and Drug Administration (FDA) for liver fibrosis grading [10]. Unlike ultrasound elastography, MRE is not limited by the presence of the skull which makes this technique also applicable to the brain [11, 12]. MRE can be used to quantify for instance neurodegenerative disease [13, 14], brain tumor malignancy [15, 16] or more recently, brain functional activity revealed by fast measurement of mechanical changes induced by neuronal activity [17].

Whatever the modality used to map the mechanical properties, shear waves have to propagate within tissue. To this end, different methods to generate mechanical waves, each with their pros and cons, have been developed which are based on external vibrating source, radiation pressure source or more recently natural source [18]. Among these methods, the external vibrating source has by far been the most used. The first reason is that it allows extracting mechanical parameters from the recorded shear wave field and not only the wavelength as done in the recently developed passive elastography [19]. The second reason is that the excitation must be compatible with the constraints and requirements of the imaging modality (space and time resolution, harmonic or transient recording etc . . .). In the case of MRI, the acquisition speed (maximum of 30 fps [20]) is much slower than it is with ultrasound (about 1,000 fps [21]). Therefore, MRI will have more capabilities to record low frequency signal generated by external driver than the transient wave generated by a radiation pressure source. On the contrary, ultrasound allow to record in real-time the propagating wave which does not imply any constraint on the type of excitation.

Overall, MRE relies on the use of an external mechanical actuator, which is challenging because of the constrained environment of the MRI system. Moreover, this actuator should be able, according to the dynamic approach of MRE (as opposed to the static approach), to generate low frequency (generally between 20 and 1,000 Hz) shear waves. Those actuators are often bulky, which burdens the use of MRI that is already a complex imaging modality to perform. Despite the high diagnosis performance of MRE [4], this technological lock prevents MRE to be democratized in clinic but also in preclinic experiment. In this challenging context, the question is: can technological progress allow designing an external mechanical actuator, as transparent as the shear wave generation is for users of ultrasound elastography? Among other vibration generators, piezoelectric ones offer interesting possibilities of integration, and miniaturization. Therefore, we propose in this paper to review the current solutions for dynamic MRE actuation using piezoelectric actuators while underlining their pros and cons compared to the other methods. Finally, flexible electroactive materials will be reviewed as they could open great perspectives to build new type of mechanical actuators for MRE.

SHEAR WAVES AS AN "*IN SITU*" BIOMECHANICAL SENSOR–SPECIFICATIONS FOR A GOOD VIBE

Local Estimation of the Stress-Strain Relationship

In general, assessment of mechanical properties relies on the measurement of the strain induced by stressing a sample. Common non-tomographic rheological methods [22, 23] applied to soft biological tissues are coarse and integrative but the stress-strain relationship is almost directly obtained from the applied stress to the sample and its resulting strain which is derived from the displacement (linear or angular) of the actuator. Assuming that the sample is homogeneous and viscoelastic, and that the mechanical stimulation stays in the linear regime, the measurement sensitivity and accuracy relies only on the hardware and its calibration. On the other side, imaging methods require to measure the stress-strain relationship locally. For MRE this is done in two steps. First, an external actuator is used to generate waves within tissues that will locally probe the mechanical response of the tissue. Then imaging of local displacement is done by synchronizing the mechanical excitation with the MRI in order to encode the wave displacement into the phase of the complex MR signal. This allows derivation of both local strain from the displacement and local stress from the second temporal derivative of the displacement. The mechanical properties can then be identified by solving the equation of motion [1]. Therefore, the accuracy of the MRE measurements depends on the quality of the mechanical excitation source, the acquisition method of the displacement map and the reconstruction algorithm used to obtain the shear modulus.

Physical and Acquisition Constraints

The ability to generate low frequency shear waves of sufficiently high amplitude (about tens of micrometers in the tissue) is mainly constrained by potential loss effects occurring within biological tissues, due to attenuation (i.e., conversion into heat) or scattering (i.e., energy getting dispersed in different directions). This attenuation increases with frequency and with tissue stiffness which may result in a rapid decrease of wave amplitude with tissue depth. In practice, this attenuation can be partially compensated by increasing the excitation amplitude but can induce, close to the mechanical actuator, heavy phase wraps, difficult to eliminate. Therefore, generating high amplitude waves is especially difficult for large and deep organs. Finally, the presence of tissue interfaces might lead to wave absorption and mode conversion. Nonlinear effects induced by varying

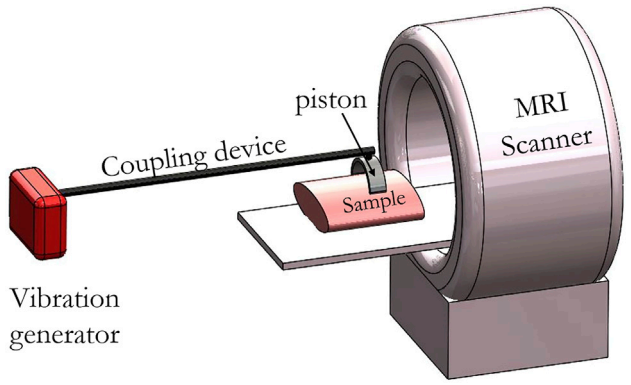

FIGURE 1 | Schematic representation of an MRE mechanical actuator positioned within the MRI machine. Generated waves are transmitted to the sample via the coupling device and a piston. Coupling devices and pistons are made of an MRI-compatible material such as plastic or PEEK for example which allows positioning inside the MRI scanner. Pistons can either fit the form of the sample, be rigid or be invasive in case of a needle. Coupling devices can be either flexible or rigid depending on the chosen material. Vibration generators are generally incompatible for usage close to an MRI scanner and have to be placed outside of the room.

preloading conditions (a beating heart, respiration etc) can influence the efficiency of high-amplitude mechanical wave transmission within biological tissues. These limitations can be overcome by a recent technique called reverberant shear wave elastography which uses multiple actuators to reinforce multi-directional waves. Unfortunately, this method is not yet available using MRI acquisition and may be limited to frequencies below 200 Hz [24].

From an acquisition point of view, the quality of MRE data can be estimated from phase to noise ratio which in a first approximation is tied to the signal to noise ratio (SNR) and the encoded phase shift [25]. Obviously the SNR will critically rely on the acquisition parameters but also on the spin transverse relaxation time (T_2^*) of the tissue that can be really low for example in liver with iron overload [26] or in lungs [27] and lead to very low SNR. Be that as it may, the encoding efficiency can be optimized by the acquisition sequence and the wave amplitude will mainly depend on physical properties and mechanical actuator settings as detailed in the following section.

Mechanical Actuator Requirements and its Characterization

As can be seen in **Figure 1**, a mechanical actuator for MRE is composed of a vibration generator which is associated with a coupling part that transmits as much as possible the mechanical excitation up to a piston which is positioned in contact with the surface of the sample. The coupling between the piston and the sample is the most difficult part of the MRE setup and has to be characterized in term of efficiency. When the vibration generator does not induce imaging artifacts, the size of the coupling device can be reduced which minimizes the associated losses. This can facilitate the integration of the mechanical actuator within the magnet bore which leads to additional free space for instruments and a greater ease of use.

The Vibration Generator

Existing vibration generators are mainly based on electromechanical (acoustic actuators can be considered as electromechanical transducers with internal magnets) and piezoelectric actuators. Electromechanical actuators are able to deliver waves of high amplitude at low frequency (10–150 Hz), are also cheaper and easier to build and to control than the piezoelectric one. However their compatibility with MRI (due to the static field (B0) distortions they induce) and related safety issues when positioned closed to the patient are problematic [28, 29]. One interesting alternative is to use a compressed air supply connected with an electromagnetic valve through a hose to control the vibration frequency and generate shear wave excitation. This approach is interesting to reduce the electrical power usually needed to generate high amplitude waves. Thereby the mechanical actuator is more MR-compatible and safe than an electromechanical one which requires higher power supply [30–32]. By comparison, piezoelectric actuators can be positioned closer to the patient without inducing image artifacts and they can work at higher frequency with high fidelity (up to 5,700 Hz) [33]. Nevertheless, this type of actuator lacks amplitude and requires amplification devices which are complex to develop. Finally, new transduction principles based on innovative materials such as optomechanical azobenzene liquid crystal open great perspectives with regards to MRI compatibility [34, 35].

Overall, the requirements for a powerful and efficient vibration generator are the following:

- A true single-frequency vibration.
- Ability to generate high amplitude displacement when loaded.
- A constant generated amplitude over a wide range of driving frequencies.
- MRI compatibility.

The Coupling Device

Due to the low MRI compatibility of most vibration generators, coupling devices are required to remotely transmit waves up to the piston. The drawback is that these coupling devices can degrade the performances of the vibration generator. The transmission lines are based on pneumatic pipes [36], rigid shaft [37–40], flexible shaft [41] or hydraulic pipes [42].

The pneumatic pipe is interesting in terms of MRI compatibility and safety as it allows easier positioning of the piston while satisfying space constraints. Nevertheless, the pneumatic transmission has low frequency accuracy (presence of harmonics) as it critically relies on the coupling with the resonant eigenmodes of the pipe. As demonstrated in [41], higher order harmonics could have an impact on the reconstruction accuracy depending on the number of cycles and the order of the harmonic. In addition to that, pneumatic pipes work mainly at low frequency (below 100 Hz), unless the extremity of the pipe is directly coupled to the sample [43, 44] or is used to actuate an unbalanced rotational mechanism [45, 46].

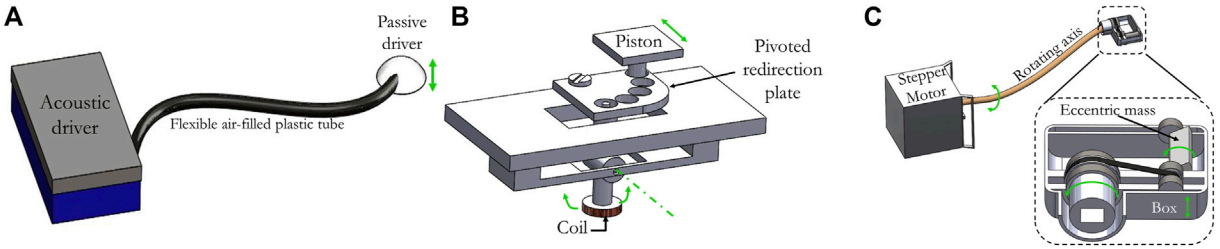

FIGURE 2 | 3D designs of three clinical actuators reported in the literature. **(A)** A pressure wave is generated by the acoustic active driver. Then the wave is transmitted through a plastic tube to a nonmetallic semi flexible membrane. To date, this is the only mechanical actuator which has been approved by the FDA and is commercially available. Depending on the application, the piston can be adapted [36]. **(B)** Displacement of the piston (green arrow) is achieved using an alternative current flowing in the coil which is placed in the static magnetic field B_0 of the MRI magnet. The coil is coupled rigidly via a revolute joint (revolution axis in green) to the frame. The pivoted redirection plate allows this actuator to provide motion of the piston in different directions unlike common electromechanical actuators [28]. **(C)** The stepper motor rotates the semi flexible PEEK rotating axis which is linked to the transducer through a locknut connection. Two PEEK rods can be found in the transducer. Those rods are glued to two PEEK timing pulleys and a timing belt. The second timing pulley is connected to a PTFE eccentric mass that induces a vertical vibration of the box. This later is positioned in contact with the sample to generate waves within the tissue. Motion direction of the different mobile parts is indicated by green arrows [41].

Recently a semi rigid coupling device has been developed using a flexible shaft made with PolyEther Ether Ketone polymer (PEEK) to transmit the mechanical wave generated by a stepper motor up to a gravitational transducer [41]. Thanks to the semi rigid coupling device, this actuator is easy to position and has a highly accurate on-resonance vibration frequency without harmonics.

The use of a hydraulic semi flexible hose allows, thanks to the incompressibility of water, better transmission than the pneumatic solution with up to a maximum of 2 mm amplitude for wave generation at the surface. This solution has been for example implemented for prostate MRE [42].

On **Figure 2,** 3D designs (Solidworks, Dassault Systèmes SE) of common clinical actuators are presented. The first actuator is an acoustic mechanical actuator with a flexible coupling device while the two others are electromechanical ones with a rigid and a semi-rigid coupling device.

The Piston

The front end of the coupling device, often called piston, requires dedicated shape and materials in order to optimize the efficient generation of shear waves within the biological tissues [47]. This piston can be actuated longitudinally which allows better penetration depth and design flexibility than with transversal actuation [47, 48]. Nevertheless, this latter generates more uniform shear waves parallel to the coupling surface. The shape of the piston is also crucial. For instance, for direct contact with soft tissues such as the breast, the efficiency of the longitudinal actuation can be enhanced by a 3D printed C-shaped breast holder with a non-planar surface to maximize the contact and potential shearing of the surface of the breast [49]. On the contrary, for indirect contact such as for the brain it is more the position of the piston relative to the skull that matters. The goal is to cause the head to experience a slight nodding motion of few microns (5–50 μm) [11, 12]. For small biological specimens it can be beneficial to generate shear waves by transversally shearing the surface of the sample to avoid bulk motion, in order to avoid the development of complex post processing tools [50]. In the case of small and fragile samples, invasive solutions have often been preferred over external actuation setups. Indeed, the latter require dedicated miniaturized actuators with a sample holder to fit potentially complex 3D shapes. Therefore several research groups have based their MRE set-up on an oscillating needle inserted along the axis of the sample which is cylindrical in this case [51–53]. Needle based actuators have also been used in interventional MRE for MRI-guided procedures [54]. Nonetheless, this invasive solution is unsatisfactory, especially as the benefit of MRI comes from its non-invasiveness.

Characterization of the MRE Actuator

The mechanical actuator can be calibrated from the vibration generator to the front end in the presence or in the absence of a load. However, the amplitude of the waves and the homogeneity of their propagation can only be checked by MRI or investigated by simulations. These simulations are also mandatory to design the coupling device and in the case of piezoelectric actuator, to design an amplification structure as done for instance in [55]. In general, characterization of the mechanical actuators have been reported either in loaded [56–59] or unloaded conditions [56, 60] mainly using a laser Doppler vibrometer. This characterization method is beneficial to characterize the frequency response of the mechanical actuator in the real condition of use. This allows one to optimize the efficiency of the setup in terms of the frequency response in order, for instance, to maximize the motion amplitude at the working frequency. Changing parts for stiffer/softer ones, or working at the eigenmodes frequencies of the setup offer simple ways to achieve the awaited specifications [61].

MRI Compatibility

One another important constraint in the design of MRE actuators is the use of materials and active electronic parts which are MRI compatible, otherwise it may result in safety issues and deleterious image artifacts during MRI examination [62]. Overall, this MRI compatibility issue is particularly problematic in MRE experiments since materials can shorten the effective transverse relaxation time (T2*) of tissues which is

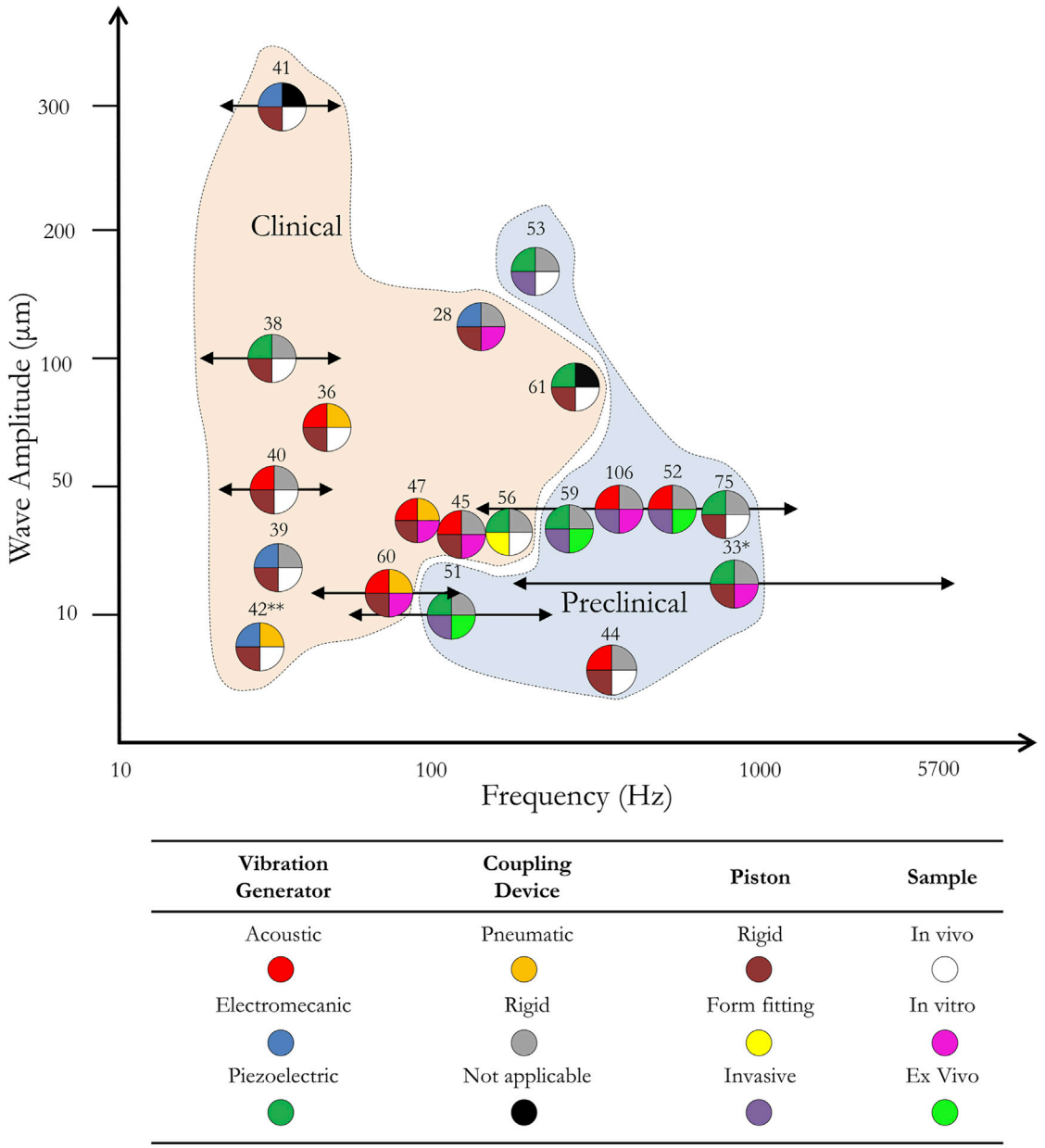

FIGURE 3 | Wave amplitude generated within the sample by mechanical actuators from the literature as a function of the frequency and the application. Each mechanical actuator is represented by a pie chart labelled by a bibliographical reference number and divided in four parts which corresponds to four actuator characteristics: the vibration generator **(top left corner)**, the coupling device **(top right corner)**, the piston **(bottom left corner)** and the type of experiment **(bottom right corner)**. Each characteristic is divided in three colored categories given in the table. The *X*-axis shows the frequency at which the MRE experiment was run, and the *Y*-axis is the wave amplitude within the region of interest. Arrows are introduced for actuators which cover a wide range of frequencies. Clinical and preclinical zones provide information on the type of application the actuators were built for. This graph only shows actuators for which both the amplitude within the tissue and the frequency information was given. (*) here, the coupling device and the piston are combined in a single part. (**) here, the pneumatic coupling device has been replaced by a hydraulic system.

not compatible with the long echo time (TE) usually required for MRE sequences.

Regarding the MRI compatibility of materials, ferromagnetic and paramagnetic materials should be avoided near the scanner, as they would experience forces and torques caused by the high magnetic fields and gradients. It would result in serious safety issues. Ferromagnetic materials must be distinguished from ferroelectric materials that have better MRI compatibility. That is why piezoelectric actuators that are mainly based on ferroelectric materials, can be positioned within the MRI scanner, closer to the sample. Nevertheless, non-magnetic and conductive materials especially metallic ones should be

positioned away from the sample as those materials can host eddy currents induced by the RF pulse and the switching magnetic field gradients. These currents may cause a significant increase of the material temperature and induce field heterogeneity which may lead to image artifacts and SNR degradation. This issue has been extensively studied and acquisition or hardware solutions have been developed to improve their MRI compatibility [63]. With regards to polymers, this type of material is highly MRI compatible even if some of them can lead to parasitic Nuclear Magnetic Resonance (NMR) signals, susceptibility artifacts or biocompatibility issues [64–66].

Another important source of safety issues and image artifacts are the active electronic parts. These have to be properly electromagnetically shielded and/or put away from the imaging region in order to avoid disturbance of the static magnetic field that would cause image artifacts. This source of artifact is particularly important for electromechanical and piezoelectric generators positioned close to the sample. A low-pass filter (cut-off frequency far below the Larmor frequency) is often necessary to limit electromagnetic coupling with RF and gradient MRI coils. Being one of the most common concerns in MRI, a standard test method has been established by the American Society for Testing and Materials (ASTM) to evaluate the MRI artifacts induced [67].

MRI Compatibility issues must be investigated only via an MRI examination. A multi gradient echo sequence with at least two echoes allows measurement of the static field map. More echoes could permit quantitative assessment of susceptibility maps [68]. Additional measurements can be necessary to quantify potential NMR signals from structures with short T2s as mentioned in [65]. Finally, degradation of the signal to noise ratio must be investigated by comparing SNR with and without the mechanical actuator.

Figure 3 graphically presents an overview of different actuators for MRE cited in the bibliography and their wave amplitude generated within the sample as a function of the working frequency. The three parts of the actuator defined previously as well as the type of sample on which the actuator has been tested are presented by a pie chart with four sections. Two areas of use of the actuator, corresponding to clinical and preclinical applications, can be identified. Overall actuators for clinical application (see **Figure 2**) are designed to work at lower frequency, i.e., below 100 Hz, than the ones for preclinical applications and can generate deep within tissues higher waves amplitude than the latter. Piezoelectric actuators offer the possibility to work at high frequencies and close to the sample which could be very beneficial to increase the mechanical coupling with small samples and integration capabilities.

As will be shown in the next sections, the use of piezoelectric actuators is justified in this case as it allows closer positioning of the vibration generator and design of a form-fitting piston without the need for a coupling device.

STATE-OF-THE-ART ON PIEZOELECTRIC ACTUATORS FOR MRE EXPERIMENTS

Piezoelectric actuators are becoming more attractive than pneumatic and electromechanical transducers because of their fast response time, their independence concerning the orientation of the static magnetic field and the low image artifacts they tend to create. In the MRE context, they have three main drawbacks: generated heat from piezoceramic stacks, the complexity of their installation and their lack of displacement amplitude. The heat dissipated by the stacks has been managed by not putting them directly on top of the patient. With regards to the installation of such actuators, one concern is the high voltages needed to supply power to the piezoelectric actuators. The actuator itself is placed within the bore of the scanner close to the patient while the power is supplied via shielded coaxial cables that go through low pass filters connected to a power amplifier located outside the scanner room. This power amplifier is generally controlled via a computer that is also located outside the scanner room. Finally, adaptations have been made to overcome the amplitude limitations either by mechanically amplifying longitudinal piezoceramic actuators or by using contracting actuators with different coupling of the actuator to the tissue. In the following subsections, the different piezoelectric materials are presented as well as their integration in a set-up dedicated for MRE which requires in some cases, a mechanical amplification device.

Basic Principles of Piezoelectric Material and Actuators

Piezoceramic actuators are usually made from Lead Zirconate Titanate (PZT), Barium Titanate ($BaTiO_3$) or Zinc Oxide (ZnO). Due to its high electromechanical coupling factor (meaning the square root of the ratio of the electrical energy output to the mechanical energy), PZT is often chosen by the industry as the main material for the commercial actuators [69, 70]. The use of piezoelectric actuators is well documented in numerous fields of engineering [70, 71]. One important drawback of piezoelectric actuators is that displacement amplitude is decreasing with the working frequencies. In order to compensate for this, currently, two types of piezoelectric actuators arrangement have emerged:

- *Piezoceramic stacks:* with longitudinal piezoelectric actuators, an electric field is applied along the polarization vector that generates a material strain. This strain is too small for MRE applications but can be increased by stacking individual actuators. Actuators would be mechanically put in series with each other while being electrically connected in parallel. With such piezoelectric assemblies, nominal displacement generally reaches around 0.10–0.15% of the initial actuator length.
- *Piezoeceramic bending elements:* They are constituted by contracting thin actuators attached to a deformable substrate. When activated, a bending moment vertical to the contraction is created. The advantage of this solution over the stack, is the larger displacement amplitudes for a smaller size but in return, the blocking force generated is much smaller which limits the application of this technology in the MRE context.

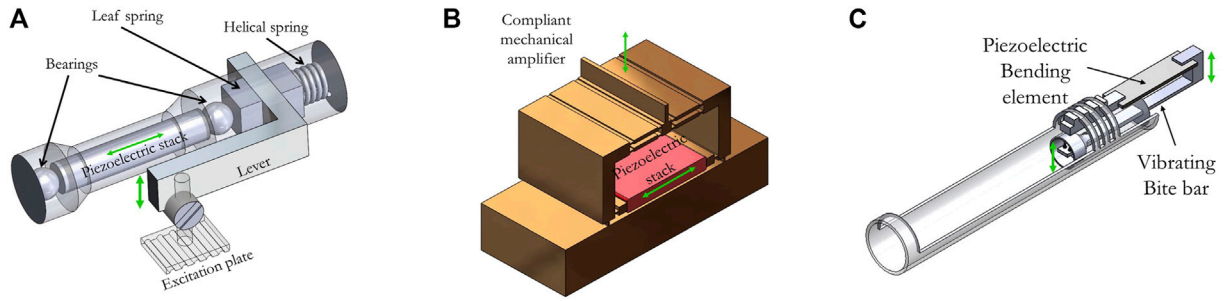

FIGURE 4 | (A) 3D designs of three piezoelectric actuators using a mechanical displacement amplifier reported in the literature. A: a brass alloy leaf spring is moved by the opposite displacement of the piezoelectric stack and a helical restoring copper-beryllium spring. This leaf spring is connected to an aluminum lever which is used, in this case, to amplify the displacement of the piezoelectric stack. The purpose of the two titanium ball bearings is to avoid shear forces on the piezoelectric stack. The displacement is transmitted to the sample via a polymethylmethacrylate excitation plate [61]. **(B)** A brass compliant mechanical amplifier (CMA) structure is used to amplify the displacement of a piezoelectric stack. The displacement is converted from longitudinal to axial by the CMA [56]. **(C)** The piezoelectric bending element vertical displacement is transmitted to the sample (mouse brain) using an L-shaped rigid copper bar [75].

To date, developing a piezoelectric actuator for MRE has not been straight forward and has required combining a piezoelectric material with a mechanical amplifier or with a bending element.

Design and Integration of Piezoelectric Actuators for MRE

Mechanically Amplified Piezoelectric Actuators

First Xu et al. [72] then Ouyang et al. [73] proposed different compliant mechanical amplifier (CMA) topologies specially designed for piezoelectric displacement amplification. The lever arm and the double asymmetric 5 bars were the ones of interest when considering MRE applications. Lever arm-based structures are the easiest CMA to construct, therefore have been extensively used in industrial applications.

As reported in [61] and illustrated in **Figure 4A**, piezoelectric stacks have been used in combination with a lever arm to transmit its displacement to the patient. In this work, the stack was a cylinder, with a diameter of 18.5 mm and a length of 247 mm. The lever was built in a way that the axial displacement of the stack is converted into a sideways motion. Numerical simulations permitted to optimize the shape of the lever and the behavior of such actuators at the frequencies of interest. The chosen T lever provided a 5-fold amplification and the amplitude of the whole actuator reached 200 μm at frequencies up to 300 Hz. Finally, materials such as aluminum, copper, and titanium were chosen as building materials for their nonmagnetic and limited artifacts properties.

Tse et al. [74] built an actuator using the same principle but with an array of 10 bimorph ceramic piezoelectric disks and an L-shape lever that provided a 3-fold amplification. This actuator reached 336 μm amplitude at 400 Hz and 278 μm at 100 Hz.

As mentioned in [61, 72, 73], lever structures are convenient to build and provide significant amplitude amplification but their topology generally presents low natural frequencies, especially when the load increases over 3 g. This issue has been tackled in two different ways.

First, Arani et al. developed a symmetric 5-bar CMA brass structure [56] that can be seen on CAD modelling in **Figure 4B**. Its advantages over the more common CMA topologies are the compactness, the absence of lateral displacement and the high natural frequency under various loads. In the laser vibrometer measurement, the CMA structure showed an amplification ratio from 10 (with a 325 g load) up to 70 (unloaded) at the respective natural frequencies ranging from 200 Hz up to 450 Hz. This paper put an emphasis on characterizing the actuator frequency response with regards to the loading. It resulted that while its natural frequency was dependent on the load in the low load regime (from no load to 240 g), its response stabilized at around 200 Hz and 240 g. The whole structure reached over 200 μm amplitude at 200 V. In the MRE experiments conducted on a gelatin phantom, the designed structure achieved a 7.6-fold amplification within the tissue mimicking phantom at a natural frequency of 200 Hz when loaded with an endorectal coil weighting 276 g. This work paved the way to reliable higher frequency MRE applications as the whole structure can be downsized, hence resulting in a higher natural frequency needed to perform MRE of small samples. Moreover, in case of high load, improving the amplification allows to reduce the input voltage which may result in a longer operating time before overheating of the stacks. This leads to additional degrees of freedom to perform the MRE acquisition.

Second, Meinhold et al. proposed a tunable resonant actuator using two mobile masses sliding on the actuator [55]. The amplified motion was perpendicular to the actuation of the ceramic. The design of this resonator was constrained by the size of the bore diameter of a small animal MRI scanner and the height of a commercially available piezoelectric stack. Two small linear piezoelectric actuators controlled the movement of the two masses between three locations: 1, 5 and 10 mm away from the center. The actuator was built in 655 silicon bronze and its dimension was determined in order to obtain a working frequency range of 680–1,117 Hz which corresponds to the high frequency range of MRE applications. The MRI compatibility of the resonator in the passive mode at a distance of 10 cm from a silicone rubber phantom was tested in a 7T scanner and showed no imaging artifacts. However, no tests have been conducted in the active mode. The proposed

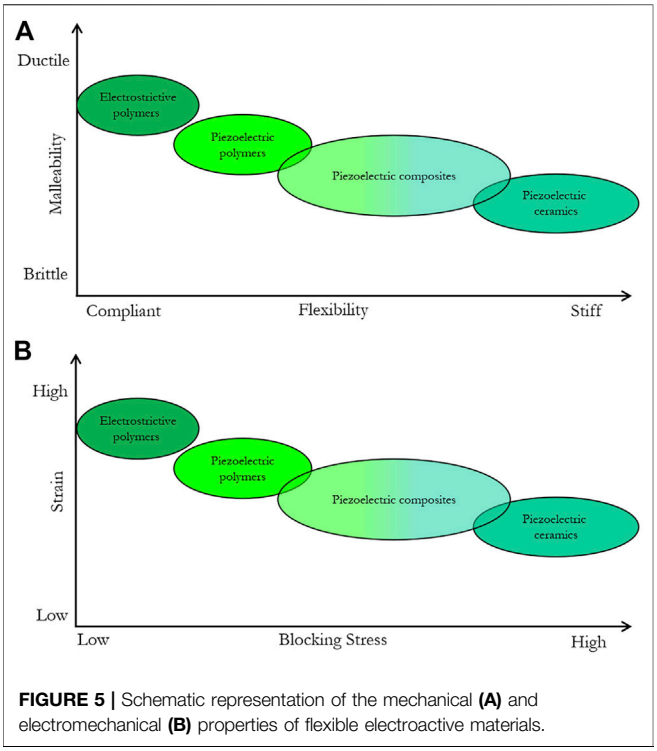

FIGURE 5 | Schematic representation of the mechanical **(A)** and electromechanical **(B)** properties of flexible electroactive materials.

actuator opens up the possibility of tuning, in the high frequency domain, an amplified actuator.

Non-amplified Piezoelectric Actuators

Using bending elements is another solution to increase the displacement amplitude of piezoelectric actuators. This relies on the bending of the tip of a bimorph piezoelectric to provide a displacement. Displacements are greater than the ones of regular longitudinal piezo ceramics. Alongside with Polyvinylidene fluoride (PVDF) films they find usage for example in low frequency energy harvester.

Chan et al. developed an actuator based on a piezoelectric bending element coupled with an acupuncture needle, produced a longitudinal motion of 200 µm without using a mechanical amplifier [53]. In this work, MRE experiments and comparison with an external driver positioned at the surface of the tissue were performed at 50, 100, 150 and 200 Hz. This work demonstrated that, compared to a surface actuator, this design allows to reduce the orientation-related error in wavelength estimation. However, the invasiveness of this actuator prevents its use for *in vivo* MRE.

Another group reported the development of an actuator for mouse brain MRE also based on a piezoelectric bending element connected to a vibrating bite bar [75]. The bite bar was made out of copper because of its rigidity and its nonmagnetic properties. The setup was mechanically characterized in loaded conditions using a laser vibrometer measurement to work at the resonance frequencies of the actuator. Taking advantage of the bending element, no mechanical amplification was needed to reach a displacement amplitude of 300 µm within a 1% agarose phantom and 30 µm within a mouse brain both at 877 Hz. A detailed view of this actuator can be seen in **Figure 4C**.

To our knowledge, bending elements have been more used in preclinical applications where the mechanical loading applied on the vibration generator is generally lower, avoiding the main drawback of this class of piezoelectric actuators: the low blocking stress which corresponds to the maximum stress generated by the actuator.

FROM PIEZOELECTRIC MATERIALS TO ELECTROACTIVE MATERIALS AND THEIR NON-MRE APPLICATIONS

Unlike electromechanical transducers, piezoelectric actuators do not suffer from any orientation limitation with regards to the static field. Nonetheless, bulk ceramic piezoelectric actuators are currently limited to a one-plane excitation and as mentioned earlier, to limited strain. One solution to this issue consists of using flexible electroactive materials to produce conformal actuators. These actuators can be made of the three following categories: piezoelectric composites, piezoelectric polymers and electrostrictive polymers. **Figure 5** presents different types of electroactive materials and their operating ranges in terms of strain vs stress and ductility vs stiffness. This graph shows that this type of new materials can allow a wide range of working domains for soft actuators from moderate stress/low displacement to low stress/high displacement. This field is rapidly evolving and, in this article, our aim is to explain their nature, the current applications and their potential for MRE. More information about basic principles and commercial application of electroactive materials can be found in [76].

Piezoelectric Composites

Piezoelectric composites have been known for a long time [77, 78]. These materials are made of a piezoelectric inorganic phase combined with a polymer matrix (in most cases not piezoelectric) [79, 80]. The goal is to combine the strong piezoelectric performances of the inorganic ceramics with the mechanical properties of polymers.

Flexible piezoelectric composites have been used as sensors for biomedical applications like the monitoring of biological low frequency signals like cardiac pulses [81–83]. Most of the studies deal with piezo sensors, but some flexible actuators have also been conceived. Dagdeviren et al [84] created a conformal array of actuators and sensors using a PZT composite for soft tissue characterization through mechanical actuation. Each actuator was made with a gold electrode and a platinum electrode deposited around a layer of nanoribbons of PZT before the whole stack was encapsulated in Polyimide. The array was designed to act simultaneously as an actuator inducing a mechanical excitation from 100 to 1,000 Hz in a tissue and a sensor able to detect small deformation at the tissue surface induced by the actuator part. In their work, the elasticity of various tissues was successfully determined. For *ex vivo* samples, both lung and heart were characterized. *In vivo*, the conformal modulus sensor was able to detect a difference in elastic modulus between a normal skin and a lesion. Arrays made of piezoelectric composite materials have also been used extensively for ultrasonic

transducers [85] and flexible transducers were designed using bulk PZT, polyimide and PDMS [86].

Piezoelectric Polymers

Ferroelectric polymers exhibit an intrinsic piezoelectric effect. There are various polymers exhibiting piezoelectricity, but the best known are mainly polymers based on PVDF and its copolymer of trifluoroethylene (PVDF-TrFE) [87], odd polyamides [88], and polymers of the polyurea [89]. However, the polymers of the PVDF (homopolymer or copolymer) have the highest piezoelectric properties and are therefore the most commonly used in applications. Using a cantilever structure based on a PVDF film, a displacement amplitude of 160 μm was reached [90] but without attempting to create vibrations. Furthermore, a bimorph actuator using two PVDF layers validated the use of such materials with a frequency range of 10 Hz-3 kHz reaching displacement amplitude of a few micrometers [91].

Electrostrictive Materials

During the last decade, much interest has been devoted to electrostrictive organic materials due to their large strain induced under electric fields, low weight, good mechanical properties, and easy processability. Electrostriction is a common phenomenon encountered in dielectric materials placed under the influence of an external electrical field that generates Maxwell stress which leads to material strain [92, 93]. Any dielectric material is electrostrictive by nature, but strain/stress effects are more pronounced in some of them. Such materials show promising potential in various applications where electromechanical conversion is required, such as low frequency energy harvesting or actuation in micropumps and artificial muscles. Despite lower generated stress than piezoelectric materials, electrostrictive polymers present high levels of electric field induced strain, more than 10-fold higher than piezoelectric fluorinated polymers at constant electric field. Among electrostrictive materials, we choose to underline two types of polymers that show, to our opinion, promising perspectives for the field of MRE actuation: Electrostrictive Polymers (EP) and Dielectric Elastomers (DE).

In addition to piezoelectricity, PVDF and its copolymers also exhibit electrostriction. However, plasticizers are needed to improve the electrostriction behavior and increase the strain that those materials can achieve [94, 95]. As an example of such EP, doped PVDF-TrFE films offer important relative strain (1–5%) under low electrical field. One example of a mechanical actuator based on EP was reported in [96] where a micropump diaphragm was developed. Quasi-constant displacement amplitude of 10–15 μm over a frequency range of 0.1–1000 Hz under high electrical field of 80V/μm was achieved. The frequency range investigated here matches the MRE one but the required electrical field could lead to image artefacts.

Interest in DE increased since Pelrine et al. reported on a commercially available acrylic elastomer able to reach a relative strain of 100% under applied voltage [97]. More theoretical details about those materials can be found in [98]. While their strain can reach higher relative values than other electroactive materials, they usually have low stresses below 10 MPa compared to a hundred of MPa for classical bulk piezoceramic. The mechanical characterizations conducted in [97] of the acrylic elastomer VHB 4910 showed a rapid decrease of strain with frequency which limits its use to low frequency actuation (tens of hertz). However, further studies showed that other material like CF19-2186 silicones can be used at higher frequencies, but with lower achievable strains. In the context of MRI, Vogan et al. [99] used an acrylic DE to reconfigure imaging coils within the bore of a scanner which illustrates both the relatively high blocking stress of those materials (up to half the maximum stress of bulk piezoceramics [100]) and the MRI compatibility of the experimental setup with a DC voltage applied to the polymer [101].

PERSPECTIVES WITH FLEXIBLE ELECTROACTIVE MATERIALS FOR MRE MECHANICAL ACTUATOR

Pros and Cons About Current Mechanical Actuators for MRE

The quality of the MRE data and elasticity estimations are dictated by the strain-to-noise ratio as explained by [102–104]. However, a mechanical actuator that can generate high wave amplitudes within the region of interest of the investigated tissue is mandatory. To our knowledge, it is unclear exactly what minimum amplitude is necessary for reconstructing an elasticity map. However, none of the actuators shown in **Figure 3** have amplitude within the tissue below 7.5 μm. In addition, the mechanical actuator should operate at a well-suited operation frequency that offers the best compromise between spatial resolution and attenuation at a given depth. This mechanical actuator should also be able to run multi-frequency experiments in order to characterize the underlying microarchitecture of the tissue from the frequency dependence of the mechanical properties [38, 52, 105, 106].

As presented in this manuscript, electromagnetic compatibility restrictions near an MRI scanner require in most cases to place the vibration generator away from the center of the scanner. Therefore, a more or less flexible and long coupling device attached to a piston is needed to transmit the vibration to the patient/sample. As illustrated in **Figure 3**, actuators based on rigid coupling devices are the most frequently used in MRE experiments thanks to their high-fidelity at high frequencies (unlike actuators based on pneumatic coupling device). Nevertheless, the supplementary loading of the coupling device limits the choice of vibration generator that can be used. Larger loudspeaker, higher currents in the case of electromechanical actuators or mechanically amplified piezoceramic stacks must be used in order to create enough displacement under such loading conditions. Thus, the vibration generator is often oversized compare to the minimum requirement which is, as mentioned previously, only to generate few microns within biological tissues. This is particularly true in case of small soft samples (i.e. mainly

samples involved in preclinical studies) and in case of superficial organs such as skin [107], breast [49] or muscle MRE [108]. In case of adult brain MRE the question is much different as the generation of wave within the brain relies on both piston-skull and skull-brain coupling. Moreover, the use of a coupling device is often associated with complicated positioning and lack of integration which can limit experimental repeatability and reproducibility.

Regarding the piston, **Figure 3** shows that most of them are rigid despite the poor sample coupling that results from it. To our knowledge few groups have design rigid form fitting piston which makes sense to access soft tissue like breast [49], but which is more questionable for the head [40, 109]. Having a flexible form-fitting piston could ensure better sample coupling, in particular when the piston is in contact with a soft surface. To our knowledge only one group reported a flexible form-fitting piston dedicated to endorectal MRE, where the piston is in contact with a soft surface [56]. In this case, an inflatable flexible piston was designed in order to fit as much as possible to the colon wall. In this case, one major drawback is that the piston-sample coupling will critically rely on tissue stiffness which make measurements intra and inter patient dependent.

As seen on **Figure 3**, most of clinical and human *in vivo* applications of MRE are in the low range of frequencies (up to 100 Hz). Looking at the wave propagation equations it appears that reaching great depth with great amplitude is easier in this range than it would be at higher frequencies. Pneumatic devices have the drawbacks of inducing phase delay and non-harmonic mechanical excitation. However, these effects are minor in the low frequency range. Moreover, pneumatic devices are the easiest to handle among different coupling devices which explains their widespread use in that frequency range. In the preclinical environment (i.e., small samples in a small-bore preclinical system) where higher frequencies are required, piezoceramic and electromechanical are the go-to solutions as shown on **Figure 3** even though they require a more complex set up than pneumatic devices. In fact, attention must be paid for instance to the following fine-tuning operations: i/cable shielding for the high voltage supply in the case of a piezoelectric vibration generator; and ii/the orientation of the electromechanical actuator with regards to the static magnetic field.

Towards Integrated and Flexible Mechanical Actuators

There is room for improvement in both clinical and preclinical MRE applications. Smaller, easier to use and more adaptable actuators could generalize the use of MRE in the MRI community. In the path towards a more optimal mechanical actuator two objectives prevail:

- Reducing the number of parts that compose the actuator in order to reduce the load on the vibration generator. A lower load would allow for low stress soft actuators to be used. A reduced number of parts would also result in more compact mechanical actuator which may simplify positioning of the MRE setup in the limited space of the MRI system.
- Using flexible form fitting pistons in order to achieve better sample coupling.

Flexible electroactive materials can be a key component of a new generation of mechanical actuators fulfilling the objectives previously exposed. As discussed above, these materials can require an electric field up to tens of V/μm in order to reach significant strain. Studying the MRI compatibility of working at such high electric fields is the first step towards reducing the number of parts for a better integration of the actuator. If the MRI compatibility of the electroactive material is validated, the piston would be the vibration generator itself without needing a coupling device. The mechanical actuator could be more compact and integrated to the MRI coil and positioned, just as a tiny patch for cardiac monitoring, directly in contact with the patient/sample. Their low blocking stress would no longer be a major issue and their compliance combined with a high strain would make them the perfect material candidate to play the role of a form-fitting mechanical actuator in contact with the patient/sample. As mentioned before, this actuation principle could work preferentially on small soft samples and in case of superficial organs. Nevertheless, to amplify the effect of such "elastography patch", one could combine such actuators in arrays to increase the penetration depth without increasing too much the applied electrical field.

To our knowledge, only [110] succeeded in building a Dielectric Elastomer (DE) and tested its MRI-compatibility on a phantom inside a 3-T MRI scanner. In their work, they started by studying the effect of the high magnetic fields produced by the scanner on the mechanical properties of their actuator and saw no difference regarding whether the actuator was inside or outside the bore of the scanner. Moreover, they also analyzed the image artifacts that their actuator would create. No SNR decrease was observed while increasing the electric field through the elastomer. Both studies helped the authors conclude that DE actuators are fully MRI-compatible and could be used in various MRI-specific applications directly in contact with a biological tissue. However, translating this work into the context of MRE would require additional measurements such as frequency response of the material as well as its achievable motion amplitude in loaded and unloaded conditions. The mechanical capabilities of the actuator were evaluated using a classical Stress/E-field curve but wave amplitude/phase and elasticity studies were not run on a phantom. Additionally, the field-induced image artifact has been characterized up to 8 V/μm and it would be interesting to see if their results remain true at higher electrical fields. Nonetheless, this work is paving the way for a broader use of this type of material in MRE.

Available Commercial Flexible Materials Suited to Design MRE Actuators

From piezoelectric composites materials to dielectric elastomers a wide range of flexible materials have been developed and optimized which make them suitable for applications in

energy harvesting, sensing and actuation. The frequency range, the strain and the stress achievable with such materials are compatible with the requirements to build MRE mechanical actuators. Moreover, the relative high "technology readiness level" (5–7 [76]) of these mechanical actuators explains the recent development of commercial solutions that could be adapted to MRE experiments.

As a matter of fact, ready to use PVDF-based transducers are commercially available (Precision acoustics, TE Connectivity, PolyK, Durham Instruments etc). However, they tend to be dedicated to ultrasonic transducing. Nonetheless, thin films of PVDF are also available from the same suppliers in order to build one's own actuators with specific sets of boundary conditions (clamping, thickness of the electrodes, stiffness of the electrodes, loading) to tailor the frequency behavior of the actuator.

Additionally, Sateco developed an actuator based on a multilayer stack of DE (silicone with carbon electrodes) with a wide operating frequency range from 0 to 2 kHz and a blocking force around 10N. The company has a starter kit with an all-in-one solution containing the actuator and all the necessary software and controllers.

After being actively involved in the field of DE [111, 112], Danfoss shut down its production of their DE solution called InLastor which could achieve an elevated blocking force of 16N, a relative strain of 2–3% and with rather low operating frequency (<100 Hz).

Another commercial solution sold by PI under the name of DuraAct is a flexible piezoelectric actuator based on a thin piezoceramic film. Custom versions with the necessary software and controllers can be ordered for specific applications such as structural health monitoring or precise actuation. The blocking force of the Power Patch model can reach 44N for a 10 μm/V relative axial deformation while working from -20 V up to 120 V.

Smart Material commercialized an alternative to the DuraAct transducers with a piezocomposite solution called Macro Fiber Composite (MFC). The M8557P1 version reaches 150 μm of axial displacement with a blocking force of 900N and an operating range of -500 V up to 1500 V with a maximum working frequency of 10 kHz. As for the previous commercial solutions, Smart Materials also provide the drivers for their actuators.

To perform MRE experiment with one of these commercial transducers will probably require a slight adaptation of the setup to be able to work in the constraint MRI environment. Particular attention must be paid to the MRI compatibility of the actuator that is often compromised by the presence of welds, electric cables and packaging parts. Fortunately, these are not always necessary for the proper operation of the actuator and can be removed with caution on a case-by-case basis.

In conclusion, recent progress made in the field of flexible electroactive materials could lead to a breakthrough in the field of actuators for MRE. These materials offer the possibility to design form-fitting actuators that are MR-compatible and can achieve relatively high displacement amplitudes with moderate blocking stresses. With few frequency limitations, they open a new path toward more adaptability, greater ease-of-use and more compactness of dedicated actuators for MRE of small soft samples and superficial organs such as skin, muscles or breast. These technological advances could be the way towards MRE experiment as easy to perform than ultrasound elastography but in 3D and with a better spatial resolution.

AUTHOR CONTRIBUTIONS

J-LG, S-AL conceived the manuscript. J-LG, J-FC, S-AL wrote the manuscript. TG, PL, VS, P-JC, MC, revised and edited the manuscript.

FUNDING

This work was supported by a grant from the Agence National de la Recherche (Estimate Project N° ANR-18-CE19-0009-01). The financial support provided by Ingénierie@Lyon, member of the Carnot Institutes Network (Metafab 3D project) for the postdoctoral scholarship of TG is also acknowledged.

ACKNOWLEDGMENTS

We thank Stuart Elliott for proofreading and improving the writing of the manuscript.

REFERENCES

1. Hirsch S, Braun J, and Sack I. *Magnetic Resonance Elastography: Physical Background and Medical Applications*. John Wiley & Sons (2016).
2. Fung YC. *Biomechanics: Mechanical Properties of Living Tissues*. 2nd ed. New York: Springer-Verlag (1993). doi:10.1007/978-1-4757-2257-4
3. Verdier C. Rheological Properties of Living Materials. From Cells to Tissues. *J Theor Med* (2003) 5:67–91. doi:10.1080/10273360410001678083
4. Mariappan YK, Glaser KJ, and Ehman RL. Magnetic Resonance Elastography: A Review. *Clin Anat* (2010) 23:497–511. doi:10.1002/ca.21006
5. Wirtz D, Konstantopoulos K, and Searson PC. The Physics of Cancer: the Role of Physical Interactions and Mechanical Forces in Metastasis. *Nat Rev Cancer* (2011) 11:512–22. doi:10.1038/nrc3080
6. Gennisson J-L, Deffieux T, Fink M, and Tanter M. Ultrasound Elastography: Principles and Techniques. *Diagn Interv Imaging* (2013) 94:487–95. doi:10.1016/j.diii.2013.01.022
7. Wang S, and Larin KV. Optical Coherence Elastography for Tissue Characterization: a Review. *J Biophoton* (2015) 8:279–302. doi:10.1002/jbio.201400108
8. Sandrin L, Fourquet B, Hasquenoph J-M, Yon S, Fournier C, Mal F, et al.Transient Elastography: a New Noninvasive Method for Assessment of Hepatic Fibrosis. *Ultrasound Med Biol* (2003) 29:1705–13. doi:10.1016/j.ultrasmedbio.2003.07.001
9. Samir AE, Dhyani M, Vij A, Bhan AK, Halpern EF, Méndez-Navarro J, et al.Shear-Wave Elastography for the Estimation of Liver Fibrosis in Chronic Liver Disease: Determining Accuracy and Ideal Site for Measurement. *Radiology* (2015) 274:888–96. doi:10.1148/radiol.14140839

10. Shire NJ, Yin M, Chen J, Railkar RA, Fox-Bosetti S, Johnson SM, et al.Test-retest Repeatability of MR Elastography for Noninvasive Liver Fibrosis Assessment in Hepatitis C. *J Magn Reson Imaging* (2011) 34:947–55. doi:10.1002/jmri.22716
11. Hiscox LV, Johnson CL, Barnhill E, McGarry MDJ, Huston J, van Beek EJR, et al.Magnetic Resonance Elastography (MRE) of the Human Brain: Technique, Findings and Clinical Applications. *Phys Med Biol* (2016) 61: R401–R437. doi:10.1088/0031-9155/61/24/R401
12. Bigot M, Chauveau F, Beuf O, and Lambert SA. Magnetic Resonance Elastography of Rodent Brain. *Front Neurol* (2018) 9:1010. doi:10.3389/fneur.2018.01010
13. Murphy MC, Huston J, and Ehman RL. MR Elastography of the Brain and its Application in Neurological Diseases. *NeuroImage* (2019) 187:176–83. doi:10.1016/j.neuroimage.2017.10.008
14. Schregel K, Wuerfel nee Tysiak E, Garteiser P, Gemeinhardt I, Prozorovski T, Aktas O, et al.Demyelination Reduces Brain Parenchymal Stiffness Quantified *In Vivo* by Magnetic Resonance Elastography. *Proc Natl Acad Sci* (2012) 109:6650–5. doi:10.1073/pnas.1200151109
15. Bunevicius A, Schregel K, Sinkus R, Golby A, and Patz S. REVIEW: MR Elastography of Brain Tumors. *NeuroImage: Clin* (2020) 25:102109–9. doi:10.1016/j.nicl.2019.102109
16. Streitberger K-J, Reiss-Zimmermann M, Freimann FB, Bayerl S, Guo J, Arlt F, et al.High-Resolution Mechanical Imaging of Glioblastoma by Multifrequency Magnetic Resonance Elastography. *PLoS One* (2014) 9: e110588. doi:10.1371/journal.pone.0110588
17. Patz S, Fovargue D, Schregel K, Nazari N, Palotai M, Barbone PE, et al.Imaging Localized Neuronal Activity at Fast Time Scales through Biomechanics. *Sci Adv* (2019) 5:eaav3816. doi:10.1126/sciadv.aav3816
18. Giammarinaro B, Zorgani A, and Catheline S. Shear-Wave Sources for Soft Tissues in Ultrasound Elastography. *IRBM* (2018) 39:236–42. doi:10.1016/j.irbm.2018.01.002
19. Zorgani A, Souchon R, Dinh A-H, Chapelon J-Y, Ménager J-M, Lounis S, et al.Brain Palpation from Physiological Vibrations Using MRI. *Proc Natl Acad Sci USA* (2015) 112:12917–21. doi:10.1073/pnas.1509895112
20. Iltis PW, Frahm J, Voit D, Joseph AA, Schoonderwaldt E, and Altenmüller E. High-speed Real-Time Magnetic Resonance Imaging of Fast Tongue Movements in Elite Horn Players. *Quant Imaging Med Surg* (2015) 5: 374–81. doi:10.3978/j.issn.2223-4292.2015.03.02
21. Tanter M, and Fink M. Ultrafast Imaging in Biomedical Ultrasound. *IEEE Trans Ultrason Ferroelect., Freq Contr* (2014) 61:102–19. doi:10.1109/TUFFC.2014.2882
22. Janmey PA, Georges PC, and Hvidt S. Basic Rheology for Biologists. In: *Methods in Cell Biology*. Elsevier (2007). doi:10.1016/S0091-679X(07)83001-9
23. Chen DTN, Wen Q, Janmey PA, Crocker JC, and Yodh AG. Rheology of Soft Materials. *Annu Rev Condens Matter Phys* (2010) 1:301–22. doi:10.1146/annurev-conmatphys-070909-104120
24. Ormachea J, and Zvietcovich F. Reverberant Shear Wave Elastography: A Multi-Modal and Multi-Scale Approach to Measure the Viscoelasticity Properties of Soft Tissues. *Front Phys* (2021) 8:606793. doi:10.3389/fphy.2020.606793
25. Yushchenko M, Sarracanie M, Amann M, Sinkus R, Wuerfel J, and Salameh N. Elastography Validity Criteria Definition Using Numerical Simulations and MR Acquisitions on a Low-Cost Structured Phantom. *Front Phys* (2021) 9:620331. doi:10.3389/fphy.2021.620331
26. Serai SD, and Trout AT. Can MR Elastography Be Used to Measure Liver Stiffness in Patients with Iron Overload? *Abdom Radiol* (2019) 44:104–9. doi:10.1007/s00261-018-1723-9
27. Marinelli JP, Levin DL, Vassallo R, Carter RE, Hubmayr RD, Ehman RL, et al.Quantitative Assessment of Lung Stiffness in Patients with Interstitial Lung Disease Using MR Elastography. *J Magn Reson Imaging* (2017) 46: 365–74. doi:10.1002/jmri.25579
28. Braun J, Braun K, and Sack I. Electromagnetic Actuator for Generating Variably Oriented Shear Waves in MR Elastography. *Magn Reson Med* (2003) 50:220–2. doi:10.1002/mrm.10479
29. Tse ZTH, Janssen H, Hamed A, Ristic M, Young I, and Lamperth M. Magnetic Resonance Elastography Hardware Design: a Survey. *Proc Inst Mech Eng H* (2009) 223:497–514. doi:10.1243/09544119JEIM529
30. Dittmann F, Tzschätzsch H, Hirsch S, Barnhill E, Braun J, Sack I, et al.Tomoelastography of the Abdomen: Tissue Mechanical Properties of the Liver, Spleen, Kidney, and Pancreas from Single MR Elastography Scans at Different Hydration States. *Magn Reson Med* (2017) 78:976–83. doi:10.1002/mrm.26484
31. Dittmann F, Reiter R, Guo J, Haas M, Asbach P, Fischer T, et al.Tomoelastography of the Prostate Using Multifrequency MR Elastography and Externally Placed Pressurized-Air Drivers. *Magn Reson Med* (2018) 79:1325–33. doi:10.1002/mrm.26769
32. Shahryari M, Tzschätzsch H, Guo J, Marticorena Garcia SR, Böning G, Fehrenbach U, et al.Tomoelastography Distinguishes Noninvasively between Benign and Malignant Liver Lesions. *Cancer Res* (2019) 79:5704–10. doi:10.1158/0008-5472.CAN-19-2150
33. Braun J, Tzschätzsch H, Körting C, Ariza de Schellenberger A, Jenderka M, and Drießle TA Compact 0.5 T MR Elastography Device and its Application for Studying Viscoelasticity Changes in Biological Tissues during Progressive Formalin Fixation. *Magn Reson Med* (2018) 79:470–8. doi:10.1002/mrm.26659
34. Clough R, Sinkus R, Holub O, and Lambert SA. *Vibration Inducing Apparatus for Magnetic Resonance Elastography*. United States patent US (2018). p. 20180172789.
35. Ceilier M, Sablong R, Faivre M, and Lambert SA. Vers Un Transducteur Opto-Mécanique Pour L'élastographie IRM? In: *Recherche en Imagerie et Technologies pour la Santé (RITS) 2017*. Lyon, France.
36. Venkatesh SK, Yin M, and Ehman RL. Magnetic Resonance Elastography of Liver: Technique, Analysis, and Clinical Applications. *J Magn Reson Imaging* (2013) 37:544–55. doi:10.1002/jmri.23731
37. Lewa CJ, Roth M, Nicol L, Franconi J-M, and de Certaines JD. A New Fast and Unsynchronized Method for MRI of Viscoelastic Properties of Soft Tissues. *J Magn Reson Imaging* (2000) 12:784–9. doi:10.1002/1522-2586(200011)12:5<784:AID-JMRI18>3.0.CO;2-Z
38. Hirsch S, Guo J, Reiter R, Papazoglou S, Kroencke T, Braun J, et al.MR Elastography of the Liver and the Spleen Using a Piezoelectric Driver, Single-Shot Wave-Field Acquisition, and Multifrequency Dual Parameter Reconstruction. *Magn Reson Med* (2014) 71:267–77. doi:10.1002/mrm.24674
39. Feng Y, Zhu M, Qiu S, Shen P, Ma S, and Zhao XA Multi-Purpose Electromagnetic Actuator for Magnetic Resonance Elastography. *Magn Reson Imaging* (2018) 51:29–34. doi:10.1016/j.mri.2018.04.008
40. Sack I, Beierbach B, Hamhaber U, Klatt D, and Braun J. Non-invasive Measurement of Brain Viscoelasticity Using Magnetic Resonance Elastography. *NMR Biomed* (2008) 21:265–71. doi:10.1002/nbm.1189
41. Runge JH, Hoelzl SH, Sudakova J, Dokumaci AS, Nelissen JL, and Guenthner CA Novel Magnetic Resonance Elastography Transducer Concept Based on a Rotational Eccentric Mass: Preliminary Experiences with the Gravitational Transducer. *Phys Med Biol* (2019) 64:045007. doi:10.1088/1361-6560/aaf9f8
42. Sahebjavaher RS, Baghani A, Honarvar M, Sinkus R, and Salcudean SE. Transperineal Prostate MR Elastography: Initial *In Vivo* Results. *Magn Reson Med* (2013) 69:411–20. doi:10.1002/mrm.24268
43. Maitre XF, Darrasse L, Sinkus R, and Louis CB. *Apparatus and Method for Generating Mechanical Waves into Living Bodies, System and Method for Mapping an Organ or Tissue and System and Method for Characterising the Mechanical Properties of Said Organ or Tissue*. United States patent US20130237807A1 (2013).
44. Salameh N, Souris L, Sarracanie M, deRochefort L, Sinkus R, Darrasse L, and Maitre XF. Feasibility of Brain MR-Elastography at 1.5 T with a Novel Wave Generator: An Animal Study. In: Proceedings of the 19th Annual Meeting ISMRM Montreal; 2011 May 7–13; QC, Canada (2011).
45. Numano T, Kawabata Y, Mizuhara K, Washio T, Nitta N, and Homma K. Magnetic Resonance Elastography Using an Air ball-actuator. *Magn Reson Imaging* (2013) 31:939–46. doi:10.1016/j.mri.2013.02.001
46. Neumann W, Schad LR, and Zollner FG. A Novel 3D-Printed Mechanical Actuator Using Centrifugal Force for Magnetic Resonance Elastography. In: Proceedings of the 39th Annual International Conference of the IEEE Engineering in Medicine and Biology Society (EMBC) Seogwipo; 2017 Jul 11–15; South Korea (2017). p. 3541–4. doi:10.1109/EMBC.2017.8037621
47. Yin M, Rouvière O, Glaser KJ, and Ehman RL. Diffraction-biased Shear Wave fields Generated with Longitudinal Magnetic Resonance Elastography

Drivers. *Magn Reson Imaging* (2008) 26:770–80. doi:10.1016/j.mri.2008.01.019
48. Kino GS. *Acoustic Waves: Devices, Imaging, and Analog Signal Processing*. Englewood Cliffs, N.J: Prentice-Hall (1987). p. 601p.
49. Bohte AE, Nelissen JL, Runge JH, Holub O, Lambert SA, de Graaf L, et al.Breast Magnetic Resonance Elastography: a Review of Clinical Work and Future Perspectives. *NMR Biomed* (2018) 31:e3932. doi:10.1002/nbm.3932
50. Connesson N, Clayton EH, Bayly PV, and Pierron F. Extension of the Optimised Virtual Fields Method to Estimate Viscoelastic Material Parameters from 3D Dynamic Displacement Fields. *Strain* (2015) 51:110–34. doi:10.1111/str.12126
51. Guertler CA, Okamoto RJ, Schmidt JL, Badachhape AA, Johnson CL, and Bayly PV. Mechanical Properties of Porcine Brain Tissue *In Vivo* and *Ex Vivo* Estimated by MR Elastography. *J Biomech* (2018) 69:10–8. doi:10.1016/j.jbiomech.2018.01.016
52. Lambert SA, Näsholm SP, Nordsletten D, Michler C, Juge L, Serfaty J-M, et al.Bridging Three Orders of Magnitude: Multiple Scattered Waves Sense Fractal Microscopic Structures via Dispersion. *Phys Rev Lett* (2015) 115:094301. doi:10.1103/PhysRevLett.115.094301
53. Chan QCC, Li G, Ehman RL, Grimm RC, Li R, and Yang ES. Needle Shear Wave Driver for Magnetic Resonance Elastography. *Magn Reson Med* (2006) 55:1175–9. doi:10.1002/mrm.20856
54. Corbin N, Vappou J, Breton E, Boehler Q, Barbé L, Renaud P, et al.Interventional MR Elastography for MRI-guided Percutaneous Procedures. *Magn Reson Med* (2016) 75:1110–8. doi:10.1002/mrm.25694
55. Meinhold W, Ozkaya E, Ueda J, and Kurt M. Tuneable Resonance Actuators for Magnetic Resonance Elastography. in Proceedings of the 2019 Design of Medical Devices Conference Minneapolis; 2019 Apr 16–18; Minnesota, USA. (2019). doi:10.1115/DMD2019-3313
56. Arani A, Eskandari A, Ouyang P, and Chopra R. A Novel High Amplitude Piezoceramic Actuator for Applications in Magnetic Resonance Elastography: a Compliant Mechanical Amplifier Approach. *Smart Mater Struct* (2017) 26:087001. doi:10.1088/1361-665X/aa71f2
57. Vappou J, Breton E, Choquet P, Willinger R, and Constantinesco A. Assessment of *In Vivo* and post-mortem Mechanical Behavior of Brain Tissue Using Magnetic Resonance Elastography. *J Biomech* (2008) 41:2954–9. doi:10.1016/j.jbiomech.2008.07.034
58. Othman SF, Xu H, Royston TJ, and Magin RL. Microscopic Magnetic Resonance Elastography (μMRE). *Magn Reson Med* (2005) 54:605–15. doi:10.1002/mrm.20584
59. Boulet T, Kelso ML, and Othman SF. Microscopic Magnetic Resonance Elastography of Traumatic Brain Injury Model. *J Neurosci Methods* (2011) 201:296–306. doi:10.1016/j.jneumeth.2011.08.019
60. Leclerc GE, Debernard L, Foucart F, Robert L, Pelletier KM, Charleux F, et al.Characterization of a Hyper-Viscoelastic Phantom Mimicking Biological Soft Tissue Using an Abdominal Pneumatic Driver with Magnetic Resonance Elastography (MRE). *J Biomech* (2012) 45:952–7. doi:10.1016/j.jbiomech.2012.01.017
61. Uffmann K, Abicht C, Grote W, Quick HH, and Ladd ME. Design of an MR-Compatible Piezoelectric Actuator for MR Elastography. *Concepts Magn Reson* (2002) 15:239–54. doi:10.1002/cmr.10045
62. Hargreaves BA, Worters PW, Pauly KB, Pauly JM, Koch KM, and Gold GE. Metal-Induced Artifacts in MRI. *Am J Roentgenol* (2011) 197:547–55. doi:10.2214/AJR.11.7364
63. Spees WM, Buhl N, Sun P, Ackerman JJH, Neil JJ, and Garbow JR. Quantification and Compensation of Eddy-Current-Induced Magnetic-Field Gradients. *J Magn Reson* (2011) 212:116–23. doi:10.1016/j.jmr.2011.06.016
64. Herrmann K-H, Gärtner C, Güllmar D, Krämer M, and Reichenbach JR. 3D Printing of MRI Compatible Components: Why Every MRI Research Group Should Have a Low-Budget 3D Printer. *Med Eng Phys* (2014) 36:1373–80. doi:10.1016/j.medengphy.2014.06.008
65. Mitsouras D, Lee TC, Liacouras P, Ionita CN, Pietilla T, Maier SE, et al.Three-dimensional Printing of MRI-visible Phantoms and MR Image-guided Therapy Simulation. *Magn Reson Med* (2017) 77:613–22. doi:10.1002/mrm.26136
66. Gerges T, Semet V, Lombard P, Gaillard S, Cabrera M, and Lambert SA. 3D Plastronics for Smartly Integrated Magnetic Resonance Imaging Coils. *Front Phys* (2020) 8:240. doi:10.3389/fphy.2020.00240
67. Woods T. MRI Safety and Compatibility of Implants and Medical Devices. *Stainl Steels Med Surg Appl* (2003) 82–9. doi:10.1520/STP11156S
68. Hwang S-h., and Lee S-K. Efficient Experimental Design for Measuring Magnetic Susceptibility of Arbitrarily Shaped Materials by MRI. *Investig Magn Reson Imaging* (2018) 22:141. doi:10.13104/imri.2018.22.3.141
69. Trolier-McKinstry S, Zhang S, Bell AJ, and Tan X. High-Performance Piezoelectric Crystals, Ceramics, and Films. *Annu Rev Mater Res* (2018) 48:191–217. doi:10.1146/annurev-matsci-070616-124023
70. Gao X, Yang J, Wu J, Xin X, Li Z, Yuan X, et al.Piezoelectric Actuators and Motors: Materials, Designs, and Applications. *Adv Mater Technol* (2020) 5:1900716. doi:10.1002/admt.201900716
71. Niezrecki C, Brei D, Balakrishnan S, and Moskalik A. Piezoelectric Actuation: State of the Art. *Shock Vib. Dig* (2001) 33:269–80. doi:10.1177/058310240103300401
72. Xu W, and King T. Flexure Hinges for Piezoactuator Displacement Amplifiers: Flexibility, Accuracy, and Stress Considerations. *Precision Eng* (1996) 19:4–10. doi:10.1016/0141-6359(95)00056-9
73. Ouyang PR, Zhang WJ, and Gupta MM. A New Compliant Mechanical Amplifier Based on a Symmetric Five-Bar Topology. *J Mech Des* (2008) 130:104501. doi:10.1115/1.2965600
74. Tse ZTH, Chan YJ, Janssen H, Hamed A, Young I, and Lamperth M. Piezoelectric Actuator Design for MR Elastography: Implementation and Vibration Issues. *Int J Med Robotics Comput Assist Surg* (2011) 7:353–60. doi:10.1002/rcs.405
75. Boulet T, Kelso ML, and Othman SF. Long-Term *In Vivo* Imaging of Viscoelastic Properties of the Mouse Brain after Controlled Cortical Impact. *J Neurotrauma* (2013) 30:1512–20. doi:10.1089/neu.2012.2788
76. Boyraz P, Runge G, and Raatz A. An Overview of Novel Actuators for Soft Robotics. *Actuators* (2018) 7:48. doi:10.3390/act7030048
77. Newnham RE, Skinner DP, and Cross LE. Connectivity and Piezoelectric-Pyroelectric Composites. *Mater Res Bull* (1978) 13:525–36. doi:10.1016/0025-5408(78)90161-7
78. Skinner DP, Newnham RE, and Cross LE. Flexible Composite Transducers. *Mater Res Bull* (1978) 13:599–607. doi:10.1016/0025-5408(78)90185-x
79. David C, Capsal J-F, Laffont L, Dantras E, and Lacabanne C. Piezoelectric Properties of Polyamide 11/NaNbO3nanowire Composites. *J Phys D: Appl Phys* (2012) 45:415305. doi:10.1088/0022-3727/45/41/415305
80. Capsal J-F, Dantras E, Dandurand J, and Lacabanne C. Electroactive Influence of Ferroelectric Nanofillers on Polyamide 11 Matrix Properties. *J Non-Crystalline Sol* (2007) 353:4437–42. doi:10.1016/j.jnoncrysol.2007.01.097
81. Ono Y, Liu Q, Kobayashi M, Jen C-K, and Blouin A. 5H-2 A Piezoelectric Membrane Sensor for Biomedical Monitoring. In: Proceedings of the 2006 IEEE Ultrasonic Symposium Vancouver; 2006 Oct 3–6; BC, Canada (2006). doi:10.1109/ULTSYM.2006.164
82. Tseng H-J, Tian W-C, and Wu W-J. Flexible PZT Thin Film Tactile Sensor for Biomedical Monitoring. *Sensors* (2013) 13:5478–92. doi:10.3390/s130505478
83. Akiyama M, Ueno N, Nonaka K, and Tateyama H. Flexible Pulse-Wave Sensors from Oriented Aluminum Nitride Nanocolumns. *Appl Phys Lett* (2003) 82:1977–9. doi:10.1063/1.1563728
84. Dagdeviren C, Shi Y, Joe P, Ghaffari R, Balooch G, Usgaonkar K, et al.Conformal Piezoelectric Systems for Clinical and Experimental Characterization of Soft Tissue Biomechanics. *Nat Mater* (2015) 14:728–36. doi:10.1038/nmat4289
85. Jung J, Lee W, Kang W, Shin E, Ryu J, and Choi H. Review of Piezoelectric Micromachined Ultrasonic Transducers and Their Applications. *J Micromech Microeng* (2017) 27:113001. doi:10.1088/1361-6439/aa851b
86. Wang Z, Xue Q-T, Chen Y-Q, Shu Y, Tian H, and Yang YA Flexible Ultrasound Transducer Array with Micro-Machined Bulk PZT. *Sensors* (2015) 15:2538–47. doi:10.3390/s150202538
87. Furukawa T, Ishida K, and Fukada E. Piezoelectric Properties in the Composite Systems of Polymers and PZT Ceramics. *J Appl Phys* (1979) 50:4904–12. doi:10.1063/1.325592
88. Capsal J-F, Dantras E, Dandurand J, and Lacabanne C. Dielectric Relaxations and Ferroelectric Behaviour of Even-Odd Polyamide PA 6,9. *Polymer* (2010) 51:4606–10. doi:10.1016/j.polymer.2010.07.040

89. Hattori T, Takahashi Y, Iijima M, and Fukada E. Piezoelectric and Ferroelectric Properties of Polyurea-5 Thin Films Prepared by Vapor Deposition Polymerization. *J Appl Phys* (1996) 79:1713–21. doi:10.1063/1.360959
90. Mahale BP, Gangal SA, and Bodas DS. PVdF Based Micro Actuator. In: Proceedings of the 1st International Symposium on Physics and Technology of Sensors (ISPTS-1); 2012 Mar 7–10; Pune, India (2012). p. 59–62. doi:10.1109/ISPTS.2012.6260878
91. Pérez R, Král M, and Bleuler H. Study of Polyvinylidene Fluoride (PVDF) Based Bimorph Actuators for Laser Scanning Actuation at kHz Frequency Range. *Sensors Actuators A: Phys* (2012) 183:84–94. doi:10.1016/j.sna.2012.05.019
92. Capsal J-F, Lallart M, Galineau J, Cottinet P-J, Sebald G, and Guyomar D. Evaluation of Macroscopic Polarization and Actuation Abilities of Electrostrictive Dipolar Polymers Using the Microscopic Debye/Langevin Formalism. *J Phys D: Appl Phys* (2012) 45:205401. doi:10.1088/0022-3727/45/20/205401
93. Lallart M, Capsal J-F, Sebald G, Cottinet P-J, and Guyomar D. Converse Electrostrictive Effect in Dielectric Polymers. *Sens Actuators B: Chem* (2014) 190:259–64. doi:10.1016/j.snb.2013.08.028
94. Della Schiava N, Le M-Q, Galineau J, Domingues Dos Santos F, Cottinet P-J, and Capsal J-F. Influence of Plasticizers on the Electromechanical Behavior of a P(VDF-TrFE-CTFE) Terpolymer: Toward a High Performance of Electrostrictive Blends. *J Polym Sci B: Polym Phys* (2017) 55:355–69. doi:10.1002/polb.24280
95. Capsal J-F, Galineau J, Lallart M, Cottinet P-J, and Guyomar D. Plasticized Relaxor Ferroelectric Terpolymer: Toward Giant Electrostriction, High Mechanical Energy and Low Electric Field Actuators. *Sens Actuators A: Phys* (2014) 207:25–31. doi:10.1016/j.sna.2013.12.008
96. Xu T-B, and Su J. Development, Characterization, and Theoretical Evaluation of Electroactive Polymer-Based Micropump Diaphragm. *Sens Actuators A: Phys* (2005) 121:267–74. doi:10.1016/j.sna.2005.01.020
97. Pelrine R, Kornbluh R, Pei Q, and Joseph J. High-Speed Electrically Actuated Elastomers with Strain Greater Than 100%. *Science* (2000) 287:836–9. doi:10.1126/science.287.5454.836
98. Carpi F, De Rossi D, Kornbluh R, Pelrine RE, and Sommer-Larsen P. *Dielectric Elastomers as Electromechanical Transducers*. Elsevier Science (2008).
99. Vogan J, Wingert A, Plante J-S, Dubowsky S, Hafez M, Kacher D, and Jolesz F. Manipulation in MRI Devices Using Electrostrictive Polymer Actuators: With an Application to Reconfigurable Imaging Coils. In: Proceedings of the 2004 International Conference on Robotics & Automation New Orleans; 2004 Apr 26–May 1; LA, USA (2004). p. 2498–504. doi:10.1109/ROBOT.2004.1307436
100. Yuan X, Changgeng S, Yan G, and Zhenghong Z. Application Review of Dielectric Electroactive Polymers (DEAPs) and Piezoelectric Materials for Vibration Energy Harvesting. *J Phys Conf Ser* (2016) 744:012077. doi:10.1088/1742-6596/744/1/012077
101. Plante J-S, Tadakuma K, DeVita LM, Kacher DF, Roebuck JR, DiMaio SP, et al.An MRI-Compatible Needle Manipulator Concept Based on Elastically Averaged Dielectric Elastomer Actuators for Prostate Cancer Treatment: An Accuracy and MR-Compatibility Evaluation in Phantoms. *J Med Devices* (2009) 3:031005. doi:10.1115/1.3191729
102. McGarry MDJ, Van Houten EEW, Perriñez PR, Pattison AJ, Weaver JB, and Paulsen KD. An Octahedral Shear Strain-Based Measure of SNR for 3D MR Elastography. *Phys Med Biol* (2011) 56:N153–N164. doi:10.1088/0031-9155/56/13/N02
103. Yue JL, Tardieu M, Julea F, Boucneau T, Sinkus R, Pellot-Barakat C, et al.Acquisition and Reconstruction Conditions In Silico for Accurate and Precise Magnetic Resonance Elastography. *Phys Med Biol* (2017) 62:8655–70. doi:10.1088/1361-6560/aa9164
104. Papazoglou S, Hamhaber U, Braun J, and Sack I. Algebraic Helmholtz Inversion in Planar Magnetic Resonance Elastography. *Phys Med Biol* (2008) 53:3147–58. doi:10.1088/0031-9155/53/12/005
105. Bigot M, Chauveau F, Amaz C, Sinkus R, Beuf O, and Lambert SA. The Apparent Mechanical Effect of Isolated Amyloid-β and α-synuclein Aggregates Revealed by Multi-frequency MRE. *NMR Biomed* (2020) 33:33. doi:10.1002/nbm.4174
106. Ronot M, Lambert SA, Wagner M, Garteiser P, Doblas S, Albuquerque M, et al.Viscoelastic Parameters for Quantifying Liver Fibrosis: Three-Dimensional Multifrequency MR Elastography Study on Thin Liver Rat Slices. *PLoS ONE* (2014) 9:e94679. doi:10.1371/journal.pone.0094679
107. Troelstra M, Polcaro A, Worsley P, Schneider T, Runge J, and Sinkus R. High-resolution One-Dimensional Shear Wave MR Elastography at 78 Microns: Initial Results in Skin Imaging *In Vivo*. In: Proceedings of the 2019 ISMRM Annual Meeting Montreal; 2019 May 11–16; QC, Canada (2019).
108. Bensamoun SF, Ringleb SI, Littrell L, Chen Q, Brennan M, Ehman RL, et al.Determination of Thigh Muscle Stiffness Using Magnetic Resonance Elastography. *J Magn Reson Imaging* (2006) 23:242–7. doi:10.1002/jmri.20487
109. Svensson SF, De Arcos J, Darwish OI, Fraser-Green J, Storås TH, Holm S, et al.Robustness of MR Elastography in the Healthy Brain: Repeatability, Reliability, and Effect of Different Reconstruction Methods. *J Magn Reson Imaging* (2021) 53:1510–21. doi:10.1002/jmri.27475
110. Carpi F, Khanicheh A, Mavroidis C, and De Rossi D. MRI Compatibility of Silicone-Made Contractile Dielectric Elastomer Actuators. *Ieee/asme Trans Mechatron* (2008) 13:370–4. doi:10.1109/TMECH.2008.924121
111. Benslimane MY, Kiil H-E, and Tryson MJ. Dielectric Electro-Active Polymer Push Actuators: Performance and Challenges. *Polym Int* (2010) 59:415–21. doi:10.1002/pi.2768
112. Tryson MJ, Sarban R, and Lorenzen KP. The Dynamic Properties of Tubular DEAP Actuators. In: Y Bar-Cohen, editor. Proceedings of SPIE - The International Society for Optical Engineering; 2010 Mar 7–11; San Diego, California, USA (2010). doi:10.1117/12.847297

Conflict of Interest: The authors declare that the research was conducted in the absence of any commercial or financial relationships that could be construed as a potential conflict of interest.